The relationships between interfacial friction and the conformational order of organic thin films

Scott S. Perry *, Seunghwan Lee, Young-Seok Shon, Ramon Colorado, Jr. and T. Randall Lee *

Department of Chemistry, University of Houston, Houston, TX 77204-5641, USA
E-mail: perry@uh.edu; trlee@uh.edu

This report describes studies of the relationships between the structures of organic monolayers and their molecular-scale frictional properties. Several distinct self-assembled monolayers (SAMs) were formed by the adsorption of a series of spiroalkanedithiols and a single structurally related normal alkanethiol. Measurements of hexadecane wettability, infrared vibrational spectroscopy, and X-ray photoelectron spectroscopy revealed that the films possessed a wide range of interfacial structures and conformational orders. Atomic force microscopy was used to measure the frictional properties of the well-characterized SAMs on the molecular scale. Comparison of the frictional data with structural information derived from complementary analytical techniques revealed a high correlation between the conformational order of the films and the observed frictional response.

KEY WORDS: self-assembled monolayers; alkanethiol; spiroalkanedithiols; gold substrates; wettability; infrared spectroscopy; X-ray photoelectron spectroscopy; AFM

1. Introduction

Over the past decade, significant progress has been made toward understanding interfacial friction on the molecular and atomic scales [1,2]. These advances have been realized through the development of analytical techniques capable of sensing forces arising from small ensembles of atoms or molecules [3,4] and the development of computational tools capable of modeling these ensembles and their interactions across an interface [5–7]. In addition, the need to understand interfacial friction on the nanometer scale has been driven by the development of technologies and products that possess nanometer-scale interfacial features and require the control of interfacial friction and wear at this level. Progress has been realized through studies of both model systems and actual devices.

For our investigations of molecular-level friction, we utilize model thin-film systems in which the composition and structure of the films can be controlled through organic synthesis and subsequently characterized by complementary surface analytical techniques. These studies have largely involved self-assembled monolayers (SAMs) derived from the adsorption of organosulfur molecules onto gold substrates. Organosulfur-based SAMs on gold have enjoyed increasing popularity both because of the ease with which the monolayers can be prepared and because of their relative stability. Our contributions in this area have involved the preparation and characterization of SAMs derived from organothiols possessing unique structures and atomic compositions. The aim of this approach has been to build into the monolayer film specifically tailored nanoscale features and compositions and then to correlate these properties with fundamental measurements of interfacial friction.

* To whom correspondence should be addressed.

Our studies have utilized SAMs composed of linear hydrocarbon chains [8], selectively fluorinated hydrocarbon chains [8–12], branched hydrocarbon chains [10], terminally functionalized (phenyl, C_{60}) hydrocarbon chains [13,14], and tethered hydrocarbon chains bound to the surface via chelating dithiol head groups [15–20]. Monolayer films generated by the adsorption of these molecules onto gold have been characterized through wettability studies using a wide range of contacting liquids, vibrational studies using polarization modulation infrared reflection absorption spectroscopy (PM-IRRAS), compositional analysis using X-ray photoelectron spectroscopy (XPS), and interfacial friction measurements using atomic force microscopy (AFM). The information gleaned from these complementary techniques has provided the unique opportunity to interpret the frictional properties of the monolayer films on a truly molecular scale.

In this paper, we present a summary of the interfacial frictional properties of a series of SAMs that differ with regard to their molecular packing on the surface and their related conformational order. A more complete description of these monolayers and their frictional properties can be found in previous publications [8–20]. Most of the molecules used to generate SAMs in this study possess the spiroalkanedithiol structure illustrated in figure 1. In the spiroalkanedithiols, two alkyl chains are connected via a quaternary carbon to two mercaptomethyl groups, which can, in turn, bind in a bidentate fashion to metal surfaces. Previous reports from our groups have detailed a wide variety of symmetrical ($R = R'$) and unsymmetrical ($R \neq R'$) spiroalkanedithiol derivatives that can be used to prepare highly stable and structurally defined SAMs on gold [15–20]. Here, we will discuss SAMs derived from only the molecules shown in figure 1. These molecules include the biden-

1023-8883/01/0300-0081$19.50/0

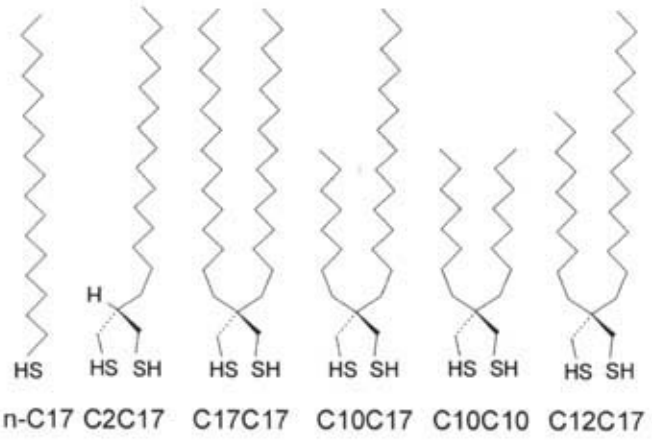

Figure 1. Illustration of the structures of the series of spiroalkanedithiols and the normal alkanethiol (n-C_{17}) used to generate SAMs in this work.

tate dithiols: 2-pentadecyl-1,3-propanedithiol (C_2C_{17}), 2-octyl-2-pentadecyl-1,3-propanedithiol ($C_{10}C_{17}$), 2-decyl-2-pentadecyl-1,3-propanedithiol ($C_{12}C_{17}$), 2,2-dipentadecyl-1,3-propanedithiol ($C_{17}C_{17}$), 2,2-dioctyl-1,3-propanedithiol ($C_{10}C_{10}$), and for comparative purposes, n-heptadecanethiol (n-C_{17}). The parenthetical abbreviations provided above will be used throughout the remainder of the paper to refer to these molecules. The adsorption of this systematic series of molecules onto gold produces SAMs in which the degree of conformational order of the alkyl chains can be controlled with remarkable precision. The degree of order arises from variations in both the chain densities and the chain lengths. A comparison of the frictional responses of these SAMs affords the unique opportunity to examine the relationships between the conformational order and the frictional properties of well-defined organic thin-film systems.

2. Experimental

The details of the synthesis and characterization of the molecules presented in figure 1 have been reported in previous publications [16–18]. Monolayers of these molecules were formed by immersing gold substrates into 1 mM isooctane solutions for 48 h. The resulting films were rinsed thoroughly with toluene and ethanol and then dried under a stream of pure nitrogen. Gold substrates for the subsequent characterization by wettability, PM-IRRAS, and XPS consisted of evaporated gold thin films on silicon substrates (evaporated gold is polycrystalline with a predominant (111) orientation [21]). For the AFM measurements, monolayers were generated on gold substrates prepared by annealing a gold wire in a H_2/O_2 flame, resulting in crystalline, (111) oriented terraces [8,22].

Advancing contact angle measurements were made using a Ramé-Hart model 100 contact angle goniometer and a Matrix Technologies micro-Electrapette 25. The drop remained in constant contact with the dispensing pipette throughout the course of these measurements. Although wettability data have been collected for a series of contacting liquids [17,19], only the results of contact angles measured between hexadecane and the SAM surfaces are presented and discussed in this report.

The vibrational spectra of the monolayer films were measured with a Nicolet MAGNA-IR 860 Fourier transform spectrometer. Data were collected in a reflection absorption mode using a Hinds Instruments PEM-90 photoelastic modulator that acted to switch between p and s polarized incident light at 37 kHz. This approach alleviates the need for background subtraction and provides high sensitivity to the molecularly thin monolayers [23–25].

A Phi model 5750 XPS spectrometer was used to measure the composition and coverage of the different monolayers. These measurements entailed integrating the intensities of the Au 4f, C 1s, and S 2p regions and deducing the relative number of chains per unit surface area from the attenuation of the gold signal. A complete description of the calibration standards, fitting procedures, and the justification of calculating film densities from XPS data can be found elsewhere [16]. The XPS data are consistent with monolayer film thicknesses measured with ellipsometry and reported elsewhere [19].

The frictional properties of the organic monolayers were determined through the simultaneous measurement of normal (load) and lateral (friction) interfacial forces with AFM. These measurements detected forces between the native oxide of a silicon nitride AFM probe tip (Digital Instruments) and the surface of the SAM. The measurements were made using a microscope based upon a beam-deflection detection scheme and a single piezoelectric tube scanner. In all of the experiments reported here, the sample was scanned with respect to a fixed tip location. The instrumentation made use of RHK AFM 100 and RHK STM 1000 electronics for the control of the sample position and detection of the cantilever motions. Interfacial frictional properties were characterized in most cases by measuring frictional forces as a function of first increasing and then decreasing load. Load data are presented in units of nN, calculated using the normal force constant of the cantiliver as provided by the manufacturer; frictional data are presented in arbitrary voltage units and simply represent an amplified photodetector response. While the lack of calibrated frictional forces precludes the estimation of coefficients of friction, all data sets presented in this paper were collected using the identical tip/cantilever assembly in order to validate comparison of the frictional properties. In a few cases, the frictional properties of the monolayers were characterized by measuring a spatially averaged frictional force at a fixed load of 0 nN. Further details of the measurements of interfacial friction using AFM have been reported elsewhere [8,26].

3. Results and discussion

3.1. Comparison of n-C_{17} and C_2C_{17}

Our first comparison of frictional response involves two thin-film systems that possess similar backbone structures

yet dissimilar packing densities. The first monolayer is that formed through the adsorption of the normal alkanethiol containing seventeen carbons, *n*-heptadecanethiol, *n*-C_{17}. The second monolayer is that formed through the adsorption of C_2C_{17}, a seventeen-carbon dithiol that bonds to the gold surface through bidentate mercaptomethyl head groups (see figure 1). In our work, normal alkanethiols have served regularly as reference markers due to their crystalline character and relatively low frictional properties [8,10,13,16,17,19]. Although a small systematic variation in friction has been observed between chains possessing odd and even numbers of carbon atoms [27], the frictional properties of the normal alkanethiol SAMs have been generally the lowest of any class of monolayer we have investigated. Moreover, normal alkanethiol SAMs having chain lengths greater than twelve carbon atoms routinely exhibit the lowest frictional responses [28–31].

Comparing the frictional properties of the well-ordered *n*-C_{17} film to those of the C_2C_{17} film provides insight into the relationships between film density and interfacial friction. It is well known that normal alkanethiols adsorb on the Au(111) surface in a $(\sqrt{3} \times \sqrt{3})$R30° orientation with the *trans*-extended alkyl chains tilted ~30° from the surface normal [32]. This adsorption geometry leads to a lattice spacing of 4.9 ± 0.2 Å, reflecting the structure and a multiple of the spacing of the underlying gold lattice. While the C_2C_{17} adsorbate also possesses a tail group that is seventeen carbons long, the propanedithiol linkage alters the adsorption geometry of the individual molecular components of the film. The formation of two gold–sulfur bonds per alkyl chain and the steric limitations associated with an apparent maximal sulfur coverage give rise to a lower chain density for the C_2C_{17} monolayer.

The existence of a lower chain density in the C_2C_{17} monolayer is substantiated through three different experimental measurements, which are summarized in table 1. First, the advancing contact angle of hexadecane (HD) measured for the C_2C_{17} film is 34°, which contrasts the value of 47° measured for the *n*-C_{17} film. The fact that the C_2C_{17} film is wet more by hexadecane suggests that the film exposes a greater number of methylene units at the liquid-film interface, which is consistent with a loosely packed liquid-like film structure.

Table 1
Relevant wettability, PM-IRRAS, and XPS data for the SAMs on gold.

Adsorbate	θ_a(HD)[a] (°)	$\nu_a CH_2$[a] (cm^{-1})	C 1s/Au 4f XPS intensity	Relative chain density[b]
n-C_{17}	47	2919	0.118	1.00
C_2C_{17}	34	2924	0.076	0.64(1)
$C_{17}C_{17}$	48	2921	0.107	0.95(1)
$C_{10}C_{17}$	<10	2927	–[c]	–
$C_{10}C_{10}$	41	2925	–	–
$C_{12}C_{17}$	27	2925	–	–

[a] Advancing contact angle values are reported with an error of ±1°, and the stretching frequencies are reported with an error of ±1 cm^{-1}.

[b] The chain density of the crystalline *n*-C_{17} monolayer is arbitrarily assigned as being a fully dense hydrocarbon layer and serves as a reference point to the other chain densities.

[c] Data not available.

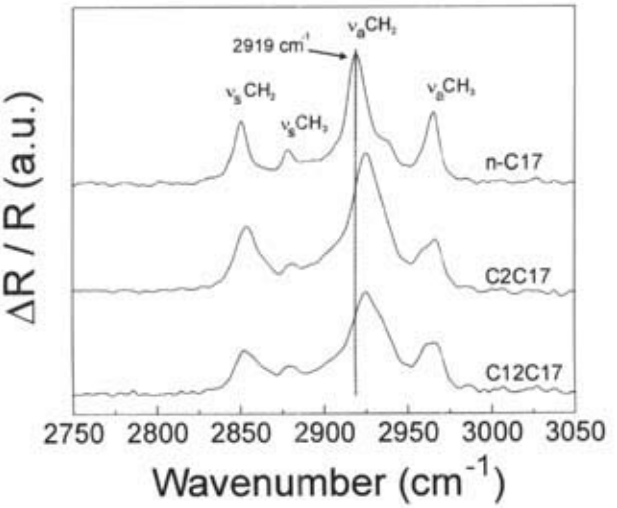

Figure 2. Polarization modulation infrared reflection absorption spectra (PM-IRRAS) for the C–H stretching region of SAMs derived from *n*-C_{17}, C_2C_{17}, and $C_{12}C_{17}$. The position of the methylene antisymmetric C–H stretch, $\nu_a CH_2$ reflects the conformational order of the monolayer, with 2919 cm^{-1} representing the value characteristic of a crystalline hydrocarbon film. Both the C_2C_{17} and $C_{12}C_{17}$ SAMs exhibit band positions substantially shifted from this value, consistent with enhanced liquid-like character within these films.

Second, the PM-IRRAS data provide direct evidence of the liquid-like character of the C_2C_{17} film. The vibrational spectra of the C–H stretching region for both films are shown in figure 2. In previous studies, the frequency and the bandwidth of the methylene antisymmetric C–H stretch, $\nu_a CH_2$, have been shown to correlate with the crystallinity or degree of conformational order of hydrocarbon polymers and thin films [22,33–35]. A stretching frequency of 2919 cm^{-1} has been measured for bulk crystalline straight-chain hydrocarbons; it is also the frequency measured in this study for the *n*-C_{17} SAM. In contrast, the C_2C_{17} film exhibits an antisymmetric methylene stretching frequency of 2924 cm^{-1}, indicating a lower degree of conformational order within the film, again consistent with a lower packing density.

Finally, quantitative differences in film density were determined through XPS measurements. Analysis of the attenuation of the photoelectrons originating from the underlying gold substrate supporting the two monolayers indicates that the chain density of the C_2C_{17} film is approximately two-thirds that of the *n*-C_{17} monolayer. This analysis considered the differing number of carbon atoms within the different adsorbates and was based upon in-house studies of a series of normal alkanethiols of different chain lengths [16]. From the fact that the measured chain density of the C_2C_{17} monolayer is greater than 50%, we infer that the number of gold–sulfur bonds formed per unit area in the C_2C_{17} SAM is greater than that formed in the *n*-C_{17} SAM. Consequently, the gold–sulfur adsorption sites for the C_2C_{17} SAM are apparently not restricted to the three-fold hollows of Au(111), as has been proposed for normal alkanethiol SAMs on gold [32].

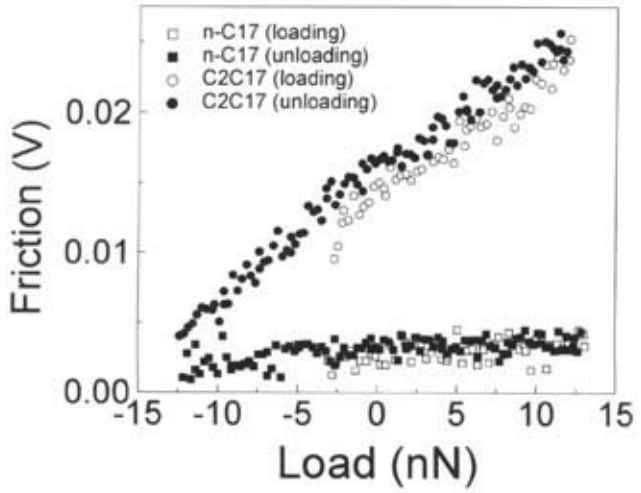

Figure 3. Friction versus load data for the n-C_{17} (□, ■) and C_2C_{17} (○, ●) SAMs measured as a function of increasing (□, ○) and decreasing (■, ●) loads. The less densely packed C_2C_{17} monolayer, although having the same chain length, exhibits a substantially higher frictional response than the crystalline n-C_{17} monolayer.

The frictional properties of the n-C_{17} and C_2C_{17} films were measured with AFM, and the data are plotted in figure 3 as a function of both increasing (empty symbols) and decreasing (filled symbols) loads. By convention, negative loads reflect adhesive forces that exist between the monolayer and the probe tip [8,26]. This effect is apparent as the decreasing load data extends to more negative loads indicating a difference in the snap-on and snap-off forces. The data shown here were collected with the identical tip/cantilever assembly and are representative of a number of measurements made in different areas of an individual film as well as measurements of independent films formed at different times. The observed differences in the frictional properties of the two films are striking: while the crystalline n-C_{17} film exhibits a consistently low frictional response, the less dense C_2C_{17} film exhibits a rapidly increasing frictional response with increasing load.

The observed frictional differences can be rationalized by considering the relative differences in film structure. As the C_2C_{17} film possesses a lower packing density, a lower elastic modulus of the film structure is expected. A lower modulus in turn leads to a greater deformation of the material per unit applied load and a relatively greater area of contact. In macroscopic systems, an increase in the area of contact with increasing load contributes to the increase in friction. While we believe that the same is true in the microscopic system studied here, we believe there is also an enhanced molecular contact between the tip and the methylene backbone units of the less dense film. This molecular-level model suggests that a greater van der Waals interaction is experienced when the tip interacts with the underlying components of the loosely packed films (1.54 Å spacing of C–C bonds) as opposed to the terminal methyl groups of densely packed films (4.99 Å lattice spacing of CH_3 groups).

The second difference in the mode of interaction between the probe tip and the film surface is related to the existing film structure. Wettability and PM-IRRAS data have shown that the n-C_{17} and C_2C_{17} SAMs exist respectively in crystalline and liquid-like states. Structurally, these data suggest a greater number of conformational defects within the C_2C_{17} film [22,33–35]. These defects are associate with the presence of C–C *gauche* conformations in the fully-extended, all-*trans* chain conformations. In addition, the lower film density should permit additional defects or conformational changes within the film as contact with the tip is made. These film deformations represent molecular channels of energy dissipation, and the higher friction observed for the C_2C_{17} film corresponds to a greater rate of energy dissipation with increasing load.

A final point of comparison between these two films involves the similar pull-off forces. In this work, the pull-off force is defined as the normal force during an unloading cycle at which the tip "snaps off" the surface, which is indicated in the data of figure 3 by the most negative load for which friction is measured. The tip is sliding during this event, and so the mechanics are different from traditional pull-off measurements. Experience, however, in our laboratory has shown that the values of pull-off forces in the presence and absence of sliding are typically indistinguishable. As a result, we take this value as a measurement of the relative adhesive interaction between the tip and contacting SAMs. From figure 3, it is apparent that, despite the different frictional properties, the two films exhibit similar adhesive interactions. This non-intuitive result is related to the deformation mechanics of the film as the tip is *withdrawn* from the monolayer and is predicted by the Johnson–Kendall–Roberts (JKR) theory of adhesion mechanics [36]. Previous experimental studies of a variety of materials in different gas and liquid environments have verified that the force of adhesion is independent of both the contact area and the elastic modulus of the contacting surfaces [37]. Thus, despite the difference in film density and the related differences in interfacial friction, the n-C_{17} and C_2C_{17} films exhibit no differences in adhesive interactions.

3.2. Comparison of $C_{17}C_{17}$, $C_{10}C_{17}$, and $C_{10}C_{10}$

The second set of monolayers to be compared consists of a series of spiroalkanedithiols of varying chain lengths. In contrast to the previous set of monolayers, all three adsorbates of this series interact with the gold surface through the bidentate nature of the dithiols and are therefore expected to possess identical molecular coverages on the surface of gold. This series includes films formed from two symmetrical adsorbates, $C_{17}C_{17}$ and $C_{10}C_{10}$, and one unsymmetrical adsorbate, $C_{10}C_{17}$ (see figure 1). Because the lengths of both alkyl chains attached to the quaternary carbon can be dictated by organic synthesis, as in the case of $C_{10}C_{17}$, we are afforded the opportunity to study homogeneously mixed monolayers having two distinct chain lengths. A previous report from our group has contrasted the properties of the homogeneously mixed monolayer to those of a monolayer composed of a mixture of the normal alkanethiols consist-

ing individually of ten and seventeen carbons [17]. While the latter were observed to phase separate on the surface, the different chains of the unsymmetrical spiroalkanedithiol adsorbate exhibited no evidence of phase separation.

The wettability of these films by hexadecane and the position of the antisymmetric methylene stretch are listed in table 1. Again, these data indicate a range of conformational orders within the films related to the molecular composition of the adsorbate. The $C_{17}C_{17}$ SAM exhibited the highest contact angle of hexadecane and the lowest antisymmetric methylene stretching frequency. While the contact angle for the $C_{17}C_{17}$ SAM is within experimental error of the value measured for the crystalline n-C_{17} SAM, the 2921 cm^{-1} $\nu_a CH_2$ stretching frequency indicates that the $C_{17}C_{17}$ SAM possesses a lower degree of conformational order. This result is consistent with our inability to obtain lattice-resolved images of the $C_{17}C_{17}$ SAM (or for SAMs formed from any of the spiroalkanedithiols) [17]. The $C_{10}C_{10}$ monolayer exhibited a slightly lower contact angle and a higher $\nu_a CH_2$ stretching frequency (2925 cm^{-1}). These results reflect an even lower degree of conformational order for the film when compared to the $C_{17}C_{17}$ film due to the shorter chain lengths and the corresponding loss of van der Waals stabilization. Finally, the $C_{10}C_{17}$ monolayer exhibited markedly different properties, being completely wet by hexadecane and exhibiting the highest value of $\nu_a CH_2$ (2927 cm^{-1}) of all the molecules examined in this report. These results indicate that the outermost portions of the film exert a substantial influence upon the interfacial properties. In the case of the $C_{10}C_{17}$ monolayer, the outermost portion of the film consists of a widely spaced seven-carbon alkyl chain. We estimate that these chains extend outward with an average spacing of 15% or more than the chains of the C_2C_{17} monolayer. The influence of the greater free volume is evident in the wettability and vibrational data as well as the frictional data described below.

As these molecules were initially investigated with regard to their structural features upon adsorption to gold [17], we neglected to collect friction-load plots (see figure 3) of the SAMs. We did, however, collect lateral force images of each of the monolayers at a fixed load of 0 nN. From these images, we then calculated spatially averaged frictional forces. Although the applied load was small for each of the images, clear differences in the frictional properties of the different films were detected. The average frictional force varied directly with the degree of conformational order: 2.8 ± 0.3 nN for the $C_{17}C_{17}$ film, 5.0 ± 0.3 nN for the $C_{10}C_{10}$ film, and 9.2 ± 0.3 nN for the $C_{10}C_{17}$ film. These values can be compared with the value obtained for the highly crystalline n-C_{17} film (2.3 ± 0.4 nN) measured using the same tip/cantilever assembly at 0 nN applied load.

Several important conclusions are evident from these results. First, the transition from a crystalline to noncrystalline monolayer structure (comparing n-C_{17} to $C_{17}C_{17}$) gives rise to a measurable difference in the frictional properties of these organic thin films. This difference is evident in the spatially averaged frictional data reported above as well as in friction–load measurements of these two films reported elsewhere [16]. In light of the identical chain lengths and approximately equal chain densities (the $C_{17}C_{17}$ monolayer possess ~95% the density of the n-C_{17} monolayer), these results indicate that higher friction correlates with the presence of a greater number of conformational defects within the film. Second, the influence of conformational order is again seen in comparing the results for the $C_{17}C_{17}$ monolayer with those of the $C_{10}C_{10}$ monolayer. Again, with similar adsorbate geometries, these films are expected to have similar surface coverages. Yet, the monolayer comprised of the shorter chain adsorbate exhibits higher friction and a more liquid-like character. These results are consistent with previous chain-length dependent studies of normal alkanethiols reported by Salmeron and coworkers, who observed decreasing friction with increasing chain length [28,29]. This phenomenon was interpreted in terms of an increasing van der Waals interaction per chain with increasing chain length and appears from the work here to be valid for both crystalline and conformationally disordered systems. Finally, we note that the friction observed for the unsymmetrical $C_{10}C_{17}$ system is approximately double that of the $C_{10}C_{10}$ system. As with the wettability and vibrational data, the frictional data indicate that the outermost portion of the film dominates the frictional interactions at low loads. The existence of higher friction in the outermost portion of the $C_{10}C_{17}$ SAM is again ascribed to the presence of numerous conformational defects (and perhaps to the creation of additional defects throughout the film during sliding). In addition, an enhanced area of contact due to a lower effective modulus is expected to contribute to the higher friction, as in the case of the C_2C_{17} monolayer.

3.3. Comparison of C_2C_{17} and $C_{12}C_{17}$

Finally, we compare two monolayer systems that possess similar frictional properties yet are structurally nonequivalent. The frictional responses of the C_2C_{17} and $C_{12}C_{17}$ SAMs are shown in figure 4 (a) (increasing load) and (b) (decreasing load). Again note that the data acquired for decreasing loads extend to more negative loads due the adhesion between the tip and sample. The most obvious conclusion from these data is that the two films exhibit identical frictional properties. Wettability studies with hexadecane (see table 1), however, indicate that the $C_{12}C_{17}$ monolayer possesses a higher fraction of exposed methylene units at the interface. This observation is consistent with a lower effective packing density arising from the extension of the C_{17} chain above the more closely packed hydrocarbon layer. The infrared data, however, indicate that the films possess approximately the same degree of conformational order (table 1 and figure 2). The similarities in the vibrational data and frictional forces observed independently for these two films strongly suggest that the overall conformational order of an organic film is perhaps the most influential factor in determining the frictional properties of compositionally similar (i.e., exclusively hydrocarbon) organic monolayers.

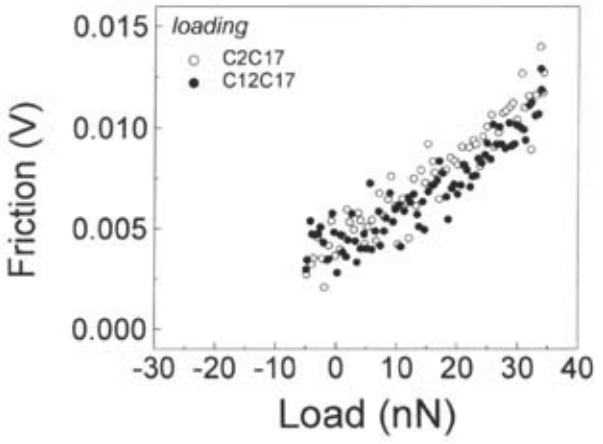

(a)

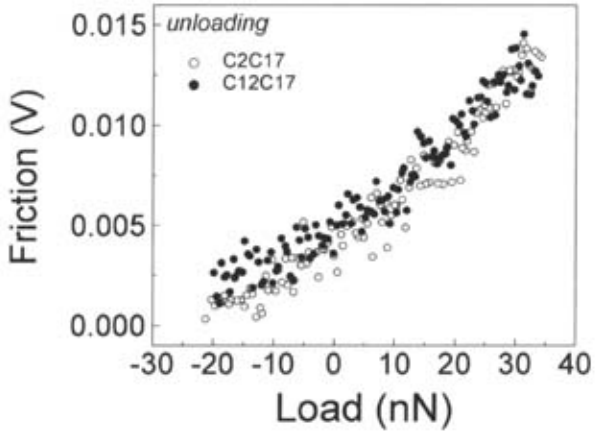

(b)

Figure 4. Friction versus load data measured for the C_2C_{17} (○) and $C_{12}C_{17}$ (●) SAMs shown for (a) increasing loads and (b) decreasing loads. Although structurally different, the two films possess similar degrees of conformational order and exhibit nearly identical frictional responses.

4. Conclusions

In this report, we have presented an investigation of the frictional properties of a series of organic monolayers possessing specific compositional and structural differences. These differences include the length of the hydrocarbon chain, the packing density of the film components, and the resulting conformational order of the hydrocarbon chains. We find a high degree of correlation between the measured frictional properties of the films and the conformational order of the films. The relationships between these two properties are defined by the mechanisms of energy dissipation in organic films, which involve a number of factors, such as the effective area of contact, the local elastic modulus, and the presence of conformational defects at a sliding interface. We also argue that organic structures that inherently possess a greater number of conformational defects at room temperature, also present lower barriers to defect creation under the action of a contacting surface and thus exhibit higher frictional properties. The quantitative assignment of the relative contributions of these largely interrelated phenomena, however, cannot be concluded from the present results and thus awaits future experimental and/or theoretical investigation [7].

Acknowledgement

This research was generously supported by the National Science Foundation (DMR-9700662 and CAREER Award to TRL: CHE-9625003) and the Robert A. Welch Foundation (Grant No. E-1320). This work made use of MRSEC Shared Experimental Facilities supported by the National Science Foundation under Award Number DMR-9632667.

References

[1] A. Ulman, Chem. Rev. 96 (1996) 1533.
[2] R.W. Carpick and M. Salmeron, Chem. Rev. 97 (1997) 1163.
[3] G. Binnig, C.F. Quate and C. Gerber, Phys. Rev. Lett. 56 (1986) 930.
[4] C.M. Mate, G.M. McCelland, R. Erlandsson and S. Chiang, Phys. Rev. Lett. 59 (1987) 1942.
[5] J.A. Harrison, C.T. White, R.J. Colton and D.W. Brenner, Phys. Rev. B 46 (1992) 9700.
[6] J.A. Harrison, C.T. White, R.J. Colton and D.W. Brenner, J. Phys. Chem. 97 (1993) 6573.
[7] A.B. Tutein, S.J. Stuart and J.A. Harrison, Langmuir 16 (2000) 291.
[8] H.I. Kim, T. Koini, T.R. Lee and S.S. Perry, Langmuir 13 (1997) 7192.
[9] H.I. Kim, T. Koini, T.R. Lee and S.S. Perry, Tribol. Lett. 4 (1998) 137.
[10] H.I. Kim, M. Graupe, G. Oluba, T. Koini, S. Imaduddin, T.R. Lee and S.S. Perry, Langmuir 15 (1999) 3179.
[11] M. Graupe, T. Koini, H.I. Kim, N. Garg, Y.F. Miura, M. Takenaga, S.S. Perry and T.R. Lee, Mater. Res. Bull. (inc. Cryst. Eng.) 34 (1999) 447.
[12] M. Graupe, T. Koini, H.I. Kim, N. Garg, Y.F. Miura, M. Takenaga, S.S. Perry and T.R. Lee, Coll. Surf. A 154 (1999) 239.
[13] S. Lee, Y.-S. Shon, T.R. Lee and S.S. Perry, Thin Solid Films 358 (2000) 152.
[14] S. Lee, M. Graupe, A. Puck, R. Colorado, Jr., Y.-S. Shon, T.R. Lee and S.S. Perry, Langmuir, submitted.
[15] Y.-S. Shon, R. Colorado, Jr., C.T. Williams, C.D. Bain and T.R. Lee, Langmuir 16 (2000) 541.
[16] S. Lee, Y.-S. Shon, R. Colorado, Jr., R.L. Guenard, T.R. Lee and S.S. Perry, Langmuir 16 (2000) 2220.
[17] Y.-S. Shon, S. Lee, S.S. Perry and T.R. Lee, J. Am. Chem. Soc. 122 (2000) 1278.
[18] R. Colorado, Jr., M. Graupe, H.I. Kim, M. Takenaga, O. Oloba, S. Lee, S.S. Perry and T.R. Lee, *Interfacial Phenomena on the Submicron Scale*, ACS Symp. Ser., in press.
[19] Y.-S. Shon, S. Lee, R. Colorado, Jr., S.S. Perry and T.R. Lee, J. Am. Chem. Soc. 122 (2000) 7556.
[20] Y.-S. Shon and T.R. Lee, J. Phys. Chem. B 104 (2000) 8182, 8192.
[21] R. Emch, J. Nogami, M.M. Dovek, C.A. Lang and C.F. Quate, J. Appl. Phys. 65 (1989) 79;
V.M. Hallmark, S. Chiang, J.F. Rabolt, J.D. Swalen and R.J. Wilson, Phys. Rev. Lett. 59 (1987) 2879;
K. Reichelt and H.O. Lutz, J. Cryst. Growth 10 (1971) 103;
M.-T. Lee, C.-C. Hsueh, M.S. Freund and G.S. Ferguson, Langmuir 14 (1998) 6419.
[22] W.A. Hayes, H. Kim, X. Yue, S.S. Perry and C. Shannon, Langmuir 13 (1997) 2511.
[23] M.R. Anderson, M.N. Evaniak and M. Zhang, Langmuir 12 (1996) 2327.
[24] M.R. Gatin and M.R. Anderson, Vib. Spectrosc. 5 (1993) 255.
[25] W.G. Golden, D.S. Dunn and J. Overend, J. Catal. 71 (1981) 395.

[26] S.S. Perry, C.M. Mate and G.A. Somorjai, Tribol. Lett. 1 (1995) 233.
[27] S.S. Wong, H. Takano and M.D. Porter, Anal. Chem. 70 (1998) 5209.
[28] X. Xiao, J. Hu, D.H. Charych and M. Salmeron, Langmuir 12 (1996) 235.
[29] A. Lio, D.H. Charych and M. Salmeron, J. Phys. Chem. B 101 (1997) 3800.
[30] R.M. Overney, E. Meyer, J. Frommer, D. Brodbeck, R. Lüthi, L. Howald, J.-J. Güntherodt, M. Fujihara, H. Takano and Y. Gotoh, Nature 359 (1992) 133.
[31] E. Meyer, R. Overney, R. Lüthi, R. Brodbeck, L. Howald, J. Frommer, H.-J. Güntherodt, O. Wolter, M. Fujihara, M. Takano and Y. Gotoh, Thin Solid Films 220 (1992) 132.
[32] A. Ulman, *An Introduction to Ultrathin Organic Films* (Academic Press, Boston, 1991).
[33] R.G. Nuzzo, L.H. Dubois and D.L. Allara, J. Am. Chem. Soc. 112 (1990) 558.
[34] R.G. Nuzzo, F.A. Fusco and D.L. Allara, J. Am. Chem. Soc. 109 (1987) 2358.
[35] F. Bensebaa, R. Voicu, L. Huron and T.H. Ellis, Langmuir 13 (1997) 5335.
[36] K.L. Johnson, *Contact Mechanics* (Cambridge University Press, Cambridge, 1985).
[37] J. Israelachvilli, *Intermolecular and Surface Forces* (Academic Press, London, 1992) pp. 326–329.